Cancer Cell, Volume *33*

Supplemental Information

Selective FcγR Co-engagement on APCs Modulates the Activity of Therapeutic Antibodies Targeting T Cell Antigens

Jeremy D. Waight, Dhan Chand, Sylvia Dietrich, Randi Gombos, Thomas Horn, Ana M. Gonzalez, Mariana Manrique, Lukasz Swiech, Benjamin Morin, Christine Brittsan, Antoine Tanne, Belinda Akpeng, Ben A. Croker, Jennifer S. Buell, Robert Stein, David A. Savitsky, and Nicholas S. Wilson

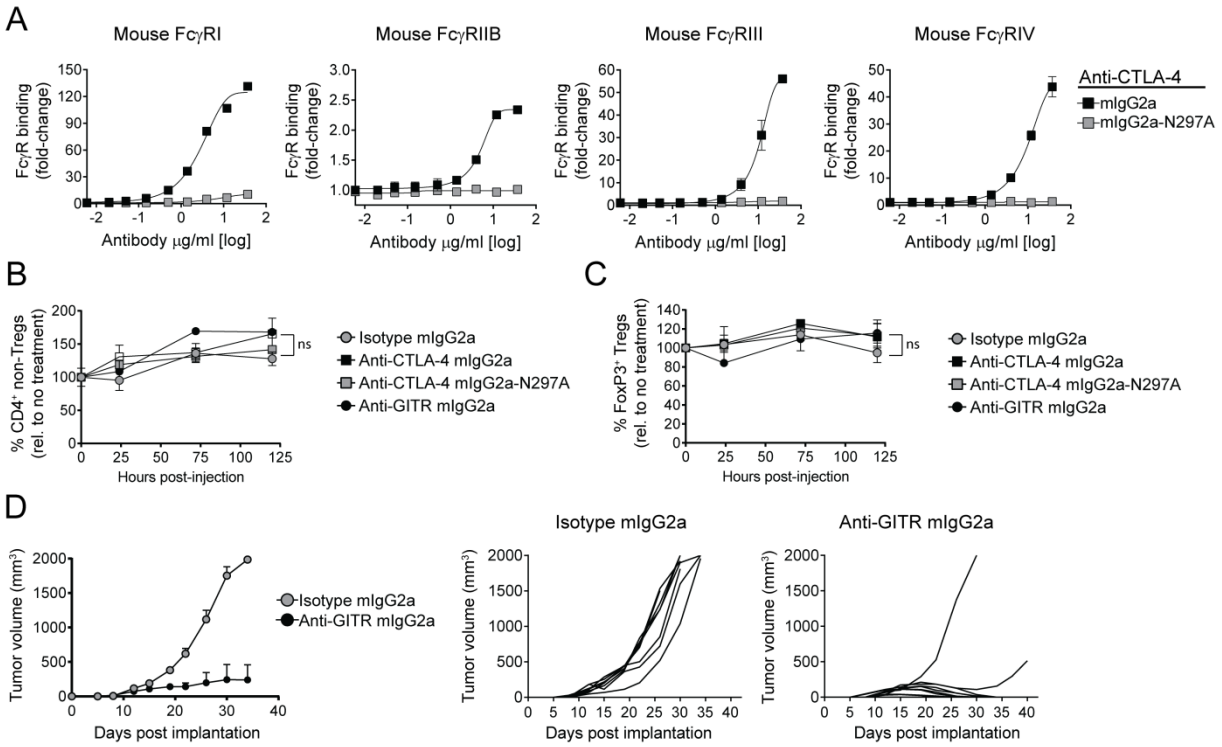

Figure S1, related to Figure 1. *In vitro* characterization of mouse FcγR binding and selectivity of intratumoral Treg cell depletion by anti-CTLA-4 mAb

(A) Binding of anti-mouse CTLA-4 mAb variants (mIgG2a or mIgG2a-N297A) to CHO cells engineered to express individual mouse Fcγ receptors. Fold-change in FcγR binding was determined by flow cytometry and calculated relative to the mean fluorescence intensity (MFI) of fluorochrome-conjugated $F(ab')_2$ secondary mAb alone.

(B, C) CT26 tumor-bearing (50-80mm^3) BALB/c mice were administered with a single 100 μg i.p. dose of anti-CTLA-4 mAb (mIgG2a or mIgG2a-N297A), anti-GITR mIgG2a, or mIgG2a isotype control mAb. Frequency of intratumoral **(B)** $CD4^+$ non-Treg cells and **(C)** tumor-draining lymph node $FoxP3^+$ Treg cells was evaluated by flow cytometry pre- (0 hr), and post-mAb injection (24, 72, and 120 hr) (n=4 mice/treatment time-point, relative to untreated control mice).

(D) BALB/c mice with established CT26 tumors (50-80mm^3) were administered with a single 100 μg i.p. dose of anti-GITR mIgG2a or mIgG2a isotype control mAb. Individual tumor growth rates (n=8-9 mice/treatment group) are shown on the right.

Data are representative of three or more experiments. A two-way ANOVA was used to calculate significance in (**B, C**). Error bars indicate SEM; ns, not significant.

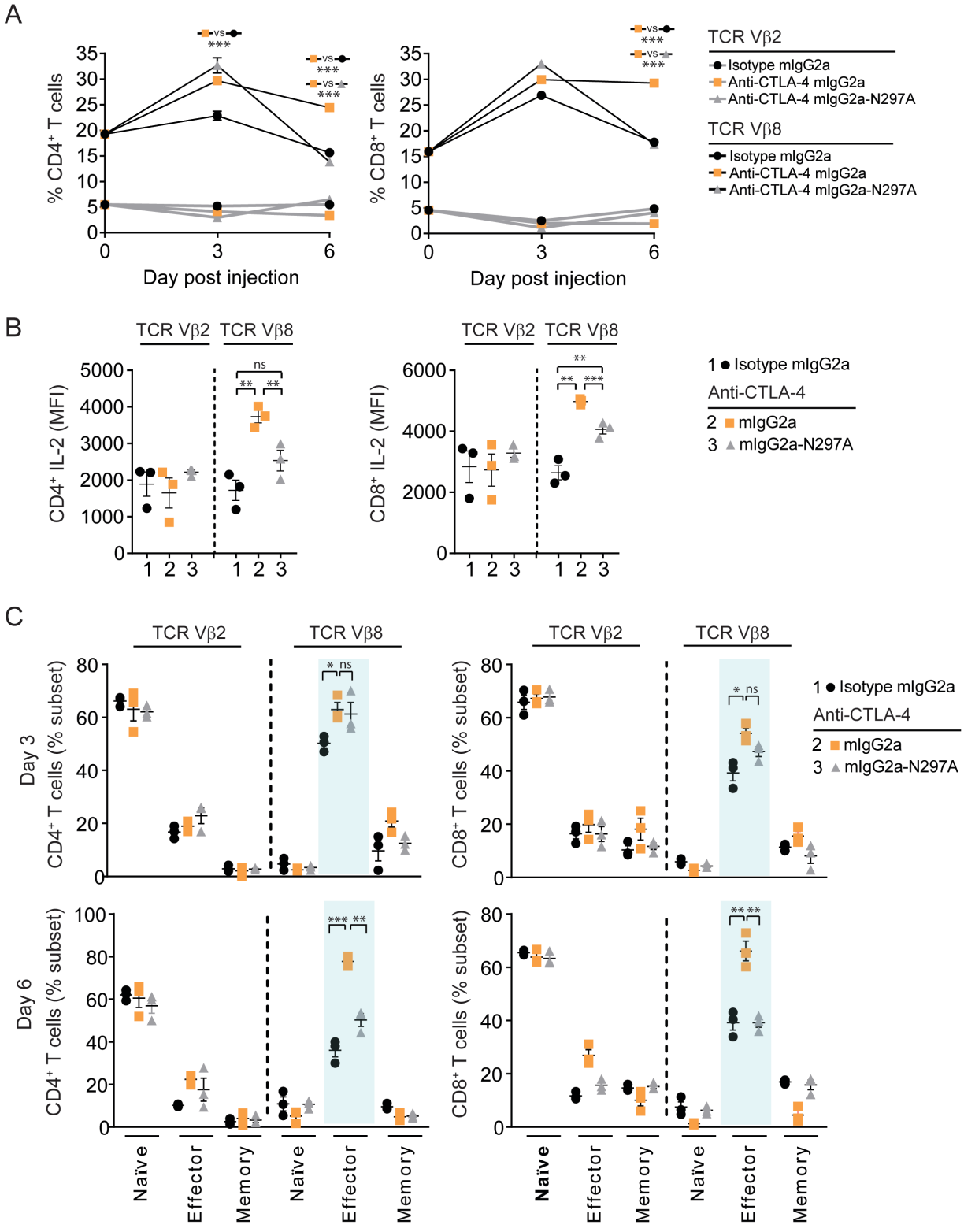
A
% CD4+ T cells
% CD8+ T cells
Day post injection
TCR Vβ2
Isotype mIgG2a
Anti-CTLA-4 mIgG2a
Anti-CTLA-4 mIgG2a-N297A
TCR Vβ8
B
CD4+ IL-2 (MFI)
CD8+ IL-2 (MFI)
Anti-CTLA-4
mIgG2a
mIgG2a-N297A
C
Day 3
Day 6
CD4+ T cells (% subset)
CD8+ T cells (% subset)
Naïve
Effector
Memory

Figure S2, related to Figure 2. FcγR co-engagement is also required for enhancement of splenic antigen-specific T cell responses by anti-CTLA-4 mAb

(A-C) C57BL/6 mice were administered i.p. with 150 μg of the SEB peptide and a separate concomitant 100 μg i.p. dose of anti-CTLA-4 mAb (mIgG2a or IgG2a-N297A) or a mIgG2a isotype control mAb (n=5 mice/group).

(A) SEB-specific (Vβ8, black lines) and non-specific (Vβ2, grey lines) splenic T cell populations were assessed on pre- (day 0) and post-treatment (day 3 and 6) by flow cytometry. A two-way ANOVA was used to calculate significance in **(A)**.

(B) IL-2 expression (MFI) by $V\beta8^+$ and $V\beta2^+$ T cells was evaluated by intracellular flow cytometry and shown for day 6 post-SEB/mAb administration.

(C) Naïve ($CD44^-$ $CD62L^+$), effector ($CD44^+$ $CD62L^-$) and memory ($CD44^+$ $CD62L^+$) T cells were evaluated on days 3 and 6 (post-treatment) by flow cytometry and represented as a percentage of total $V\beta8^+$ or $V\beta2^+$ T cells.

Data are representative of three or more experiments. A Student's t test was used to calculate significance in (**B, C**). Error bars indicate SEM; ns, not significant; *, $p<0.05$; $p<0.01$; ***, $p< 0.001$.

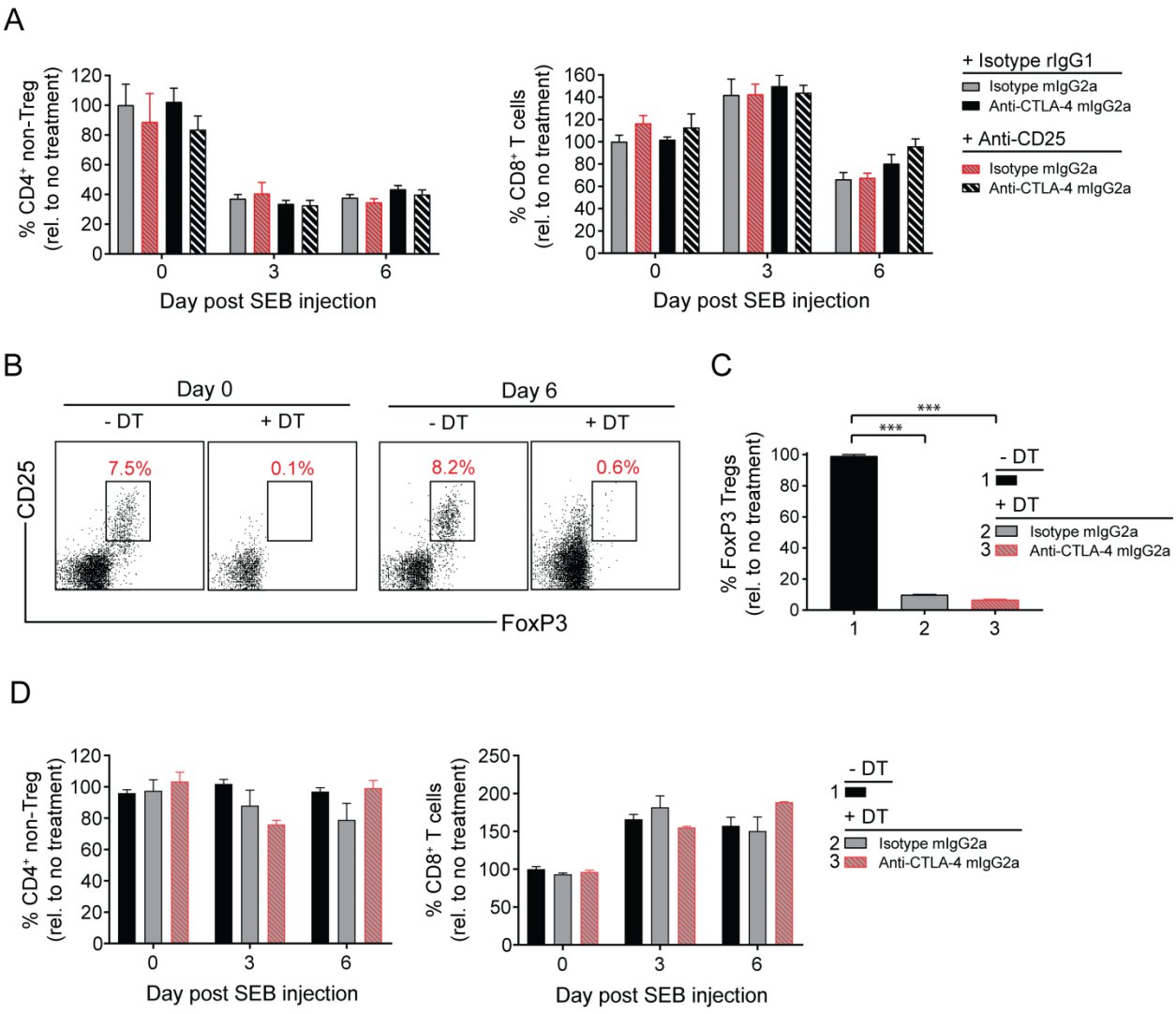

Figure S3, related to Figure 3. Anti-CD25 mAb- and FoxP3^{DTR}-mediated depletion is potent and selective for Treg cells

(A) On day -10, C57BL/6 mice were administered with a single i.p. 250 μg dose of anti-CD25 mAb (clone PC61). On Day 0, mice were administered with separate i.p. injections SEB and anti-CTLA-4 mIgG2a mAb (n=4 mice/group). The frequency of CD4$^+$ non-Treg cell and CD8$^+$ T cell populations in control and anti-CD25 mAb-treated mice pre- (day 0) and post-SEB/mAb injection (days 3 and 6) was assessed in the peripheral blood by flow cytometry.

(B-D) FoxP3^{DTR} mice were administered with 100 μg i.p. of diphtheria toxin (DT) on days -2 and -1 to systemically deplete FoxP3-expressing Treg cells.

(B) Representative flow cytometry plots of FoxP3$^+$ Treg cells from the peripheral blood of FoxP3^{DTR} mice pre- (day 0) and post-SEB/mAb injection (day 6).

(C) Frequency of FoxP3$^+$ Treg cells in DT treated and untreated (normalized to 100%) FoxP3^{DTR} mice pre- (day 0) and post-SEB/mAb injection (day 6) was assessed in the spleen by flow cytometry.

(D) Frequency of $CD4^+$ non-Treg cell and $CD8^+$ T cell populations in DT treated and untreated (normalized to 100%) $FoxP3^{DTR}$ mice pre- (day 0) and post-SEB/mAb injection (days 3 and 6) was assessed in the peripheral blood by flow cytometry.
Data are representative of three or more experiments. A Student's t test was used to calculate significance in **(C)**. Error bars indicate SEM; ***$p< 0.001$.

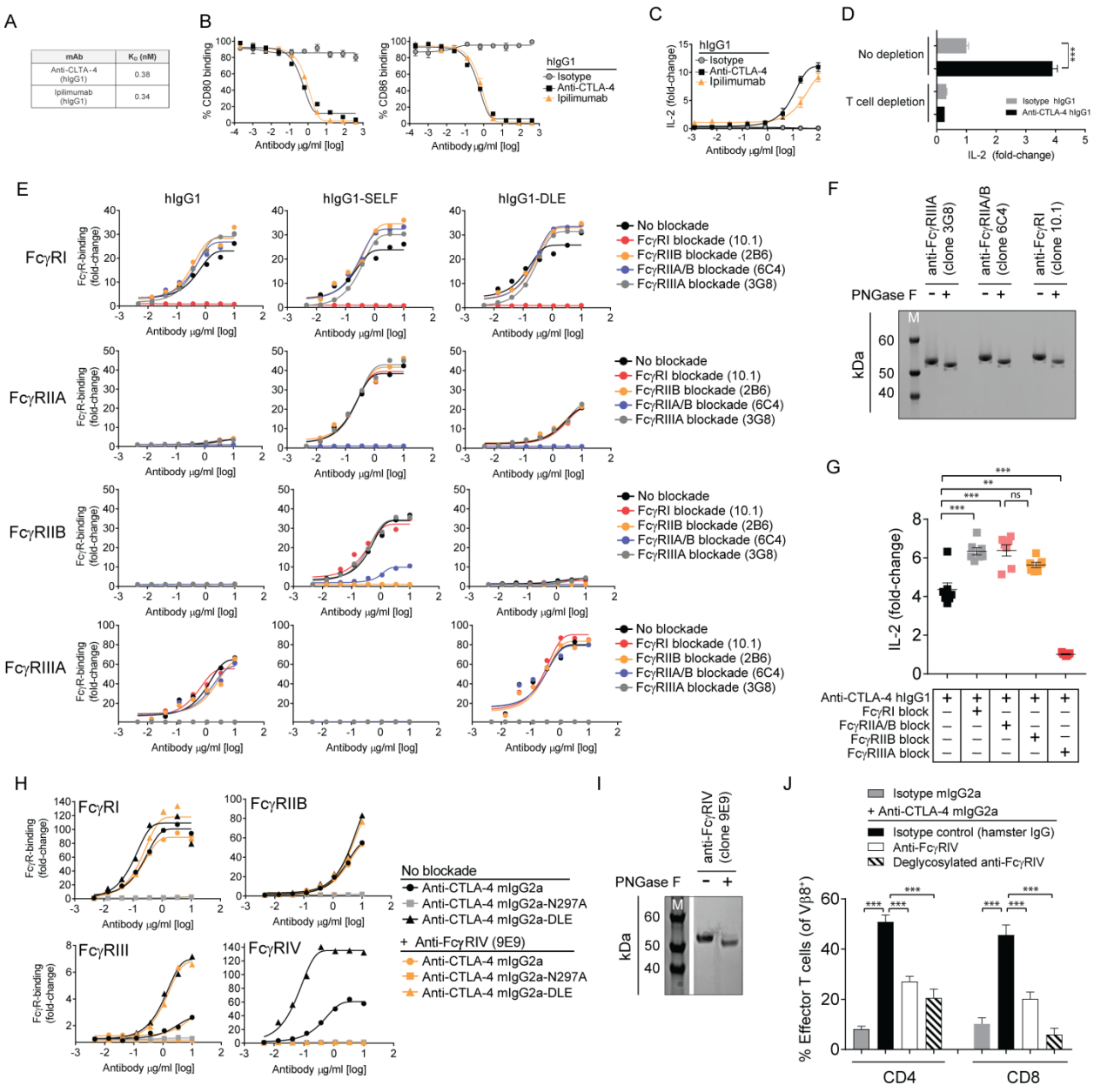

Figure S4, related to Figure 4. Characterization of CTLA-4 mAbs and FcγR blocking antibodies.

(A) Surface plasmon resonance (SPR)-based affinity assessment of anti-human CTLA-4 mAb and ipilimumab to recombinant human CTLA-4 protein (dimeric, Fc-fusion).

(B) Blockade of the CTLA-4 binding to CD80 and CD86 with increasing concentrations of anti-CTLA-4 mAb, ipilimumab, or isotype control (hIgG1).

(C) IL-2 production (day 4) from human PBMCs stimulated with 100 ng/ml of SEA peptide and increasing concentrations of anti-CTLA-4 mAb, ipilimumab, or isotype control (hIgG1).

(D) IL-2 production (day 4) from PBMCs with or without depletion of T cells following stimulation with SEA peptide and anti-CTLA-4 hIgG1 or isotype control mAb (10 µg/ml).

(E) Binding of anti-human CTLA-4 mAb variants (hIgG1, hIgG1-DLE, and hIgG1-SELF) to CHO cells expressing different human Fcγ with or without pre-blockade using specific deglycosylated FcγR blocking antibodies (10 μg/ml of anti-FcγRIIA/B clone 6C4, -FcγRIIIA clone 3G8, or agylcosylated anti-FcγRIIB clone 2B6; 20 μg/ml was used for anti-FcγRI clone 10.1). Fold-change in FcγR binding was determined by flow cytometry and calculated relative to the MFI of fluorochrome-conjugated $F(ab')_2$ secondary mAb alone **(E** and **H)**.
(F) Anti-human FcγR-specific mAbs were deglycosylated with PNGase F. To visualize glycosylation-dependent band shifts of the IgG heavy chain, samples were evaluated by reducing SDS-PAGE. The aglycosylated anti-human FcγRIIB antibody (mIgG2a-N297A, clone 2B6) was excluded from PNGase F treatment. M refers to marker ladder.
(G) IL-2 production (day 4) by PBMCs stimulated with SEA peptide (100 ng/ml) and anti-CTLA-4 hIgG1 (10 μg/ml) with or without blockade of select Fcγ receptors with deglycosylated anti-FcγR mAbs.
(H) Binding of anti-mouse CTLA-4 mAb variants (mIgG2a, mIgG2a-N297A, and mIgG2a-DLE) to CHO cells expressing different mouse Fcγ receptors (FcγRI, IIB, III, and IV) with or without pre-blockade by deglycosylated FcγRIV-specific mAb (clone 9E9, 10 μg/ml).
(I) Anti-mouse FcγRIV-specific mAb was deglycosylated with PNGase F. Glycosylation-dependent band shifts of the IgG heavy chain were evaluated by reducing SDS-PAGE.
(J) C57BL/6 mice were given sequential i.p. injections of glycosylated or deglycosylated anti-FcγRIV mAb (clone 9E9) or a hamster IgG isotype control (200 μg), together with SEB peptide (150 μg) and anti-CTLA-4 mIgG2a or isotype control mAb (100 μg) (n=4 mice). The frequency of $V\beta8^+$ effector ($CD44^+$ $CD62L^-$) T cells was evaluated on day 6 by flow cytometry.
Fold-change in IL-2 was calculated relative to a no mAb control **(C**, **D**, and **G)**. Data are representative of three or more experiments. A Student's t test was used to calculate significance in **(D, G,** and **J)**. Error bars indicate SEM; ns, not significant; **, $p<0.01$; ***, $p< 0.001$.

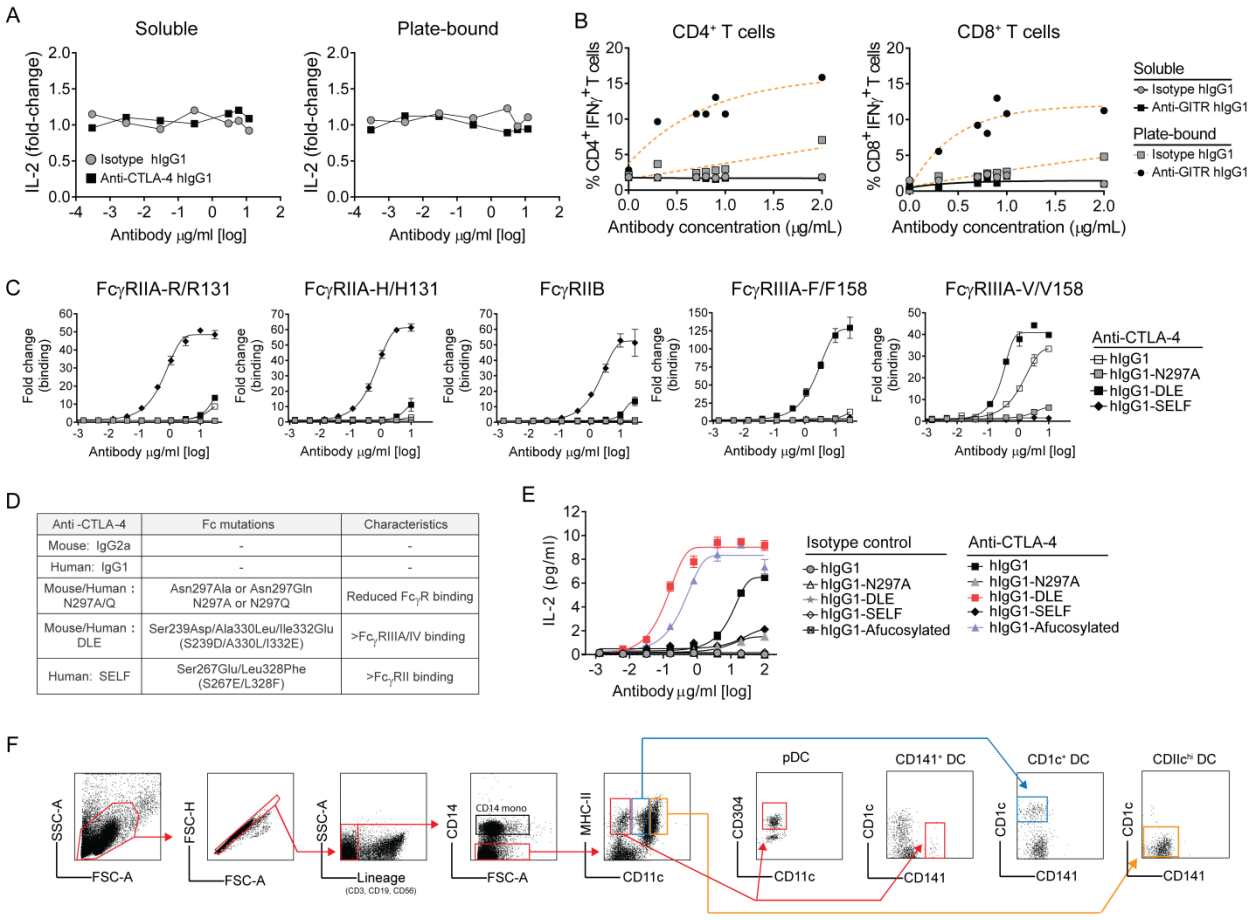

D

Anti -CTLA-4	Fc mutations	Characteristics
Mouse: IgG2a	-	-
Human: IgG1	-	-
Mouse/Human : N297A/Q	Asn297Ala or Asn297Gln N297A or N297Q	Reduced $Fc_\gamma R$ binding
Mouse/Human : DLE	Ser239Asp/Ala330Leu/Ile332Glu (S239D/A330L/I332E)	>Fc_γRIIIA/IV binding
Human: SELF	Ser267Glu/Leu328Phe (S267E/L328F)	>Fc_γRII binding

G

Healthy donor peripheral blood

			FcγRI		FcγRIIB		FcγRIIA		FcγRIIIA	
	Population	% of CD14+	% of Total PBMCs	% of CD14+	% of Total PBMCs	% of CD14+	% of Total PBMCs	% of CD14+	% of Total PBMCs	% of CD14+
Live, Lineage negative	CD14 mono	100	5.8	41	3.9	22	13	91	0.6	4.7

			FcγRI		FcγRIIB		FcγRIIA		FcγRIIIA	
	Population	% of CD14-	% of Total PBMCs	% of DC population	% of Total PBMCs	% of DC population	% of Total PBMCs	% of DC population	% of Total PBMCs	% of DC population
Live, Lineage negative CD14-	CD1c+ DC	1.4 ± 0.9	0.01	0.44	0.01	0.01	0.2	92	0.01	0.01
	CD141+ DC	0.03 ± 0.01	0.01	0.12	0.01	0.01	0.01	72	0.01	0.01
	pDC	0.8 ± 0.5	0.01	0.21	0.01	0.01	0.01	66	0.01	0.01
	CD11c hi DC	4.4 ± 3.4	0.01	0.64	0.06	12	0.6	88	0.5	81

Figure S5, related to Figure 5. Additional characterization of anti-human CTLA-4 mAb Fc variants and analysis of human PBMC FcγR expression.

(A, B) T cells were isolated from human PBMCs and stimulated with anti-CD3 mAb (5 μg/ml) in combination with increasing concentrations of plate-bound (cross-linked) or soluble anti-CTLA-4 hIgG1, anti-GITR hIgG1, or a hIgG1 isotype control mAbs.

(A) IL-2 production (on day 4) from T cells treated with soluble or plate-bound anti-CTLA-4 mAb or hIgG1 isotype control.

(B) IFNγ production (day 3 post-mAb treatment) from anti-GITR hIgG1- or isotype hIgG1-treated $CD4^+$ and $CD8^+$ T cells was quantitated by intracellular flow cytometry.

(C) Binding of anti-human CTLA-4 mAb variants (hIgG1, hIgG1-N297A, hIgG1-SELF, and hIgG1-DLE) to CHO cells engineered to express human FcγRs. Fold-change in FcγR binding

was determined by flow cytometry and calculated relative to the MFI of fluorochrome-conjugated $F(ab')_2$ secondary mAb alone.
(D) Summary of mAb Fc variant modifications and associated FcγR binding characteristics.
(E) IL-2 production (on day 4) by human PBMCs stimulated with 100 ng/ml of SEA peptide together with increasing concentrations of anti-CTLA-4 mAb variants (hIgG1, hIgG1-N297A, hIgG1-DLE, hIgG1-SELF, hIgG1-Afucosylated) or corresponding hIgG1 isotype control mAbs.
(F) Representative flow cytometry plots illustrating the gating used to identify DC ($CD1c^+$, $CD141^+$, $CD304^+$ (plasmacytoid DC, pDC)) and $CD14^+$ monocyte subsets from human PBMCs. Here "lineage negative" refers to $CD3^-$ $CD19^-$ $CD56^-$ cells.
(G) Percentage of $Fc\gamma R^+$ monocyte (lineage negative $CD14^+$) and DC (lineage negative $CD14^-$) subsets. Percent populations are of total PBMCs or of the indicated DC subset gates.
Fold-change in IL-2 was calculated relative to a no mAb control (**A** and **E**). Data are representative of three or more experiments. Error bars indicate SEM.

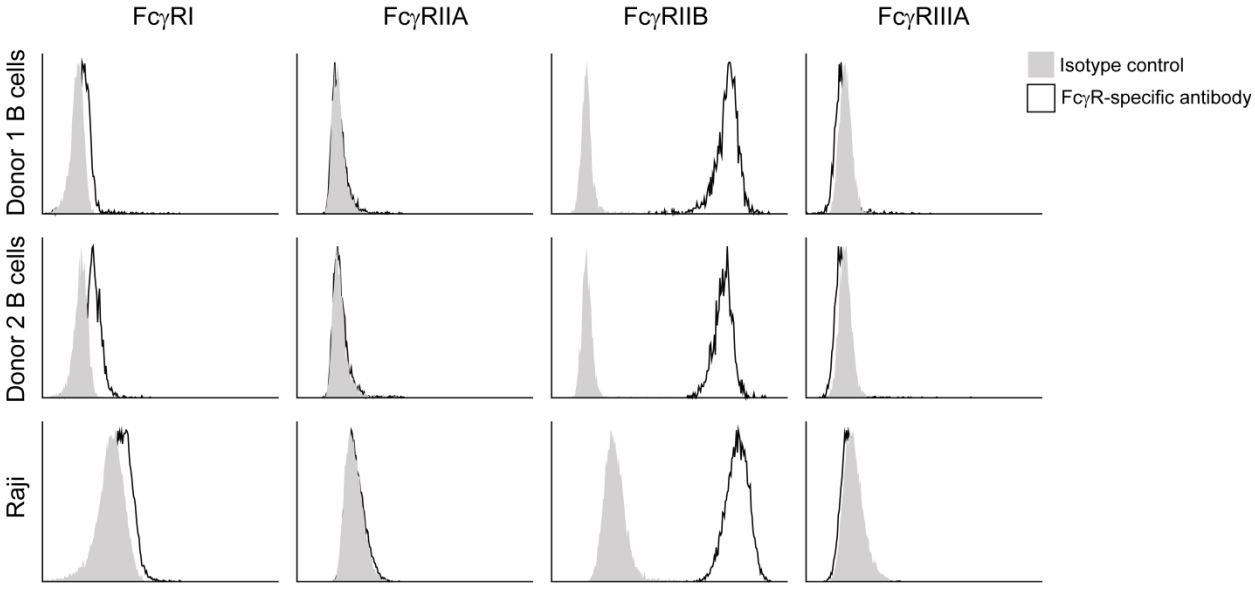

Figure S6, related to Figure 6. Comparison of human B cell and Raji FcγR expression
Representative flow cytometry profiles of FcγRs on human PBMC-derived $CD3^-$ $CD20^+$ B cells and Raji cells. Data are representative of three or more experiments and a minimum of three separate donor samples.